Contribution from the Department of Inorganic Chemistry,
Indian Association for the Cultivation of Science, Calcutta 700032, India

Ruthenium and Osmium Complexes of N,O Chelators: Syntheses, Oxidation Levels, and Distortion Parameters

Goutam Kumar Lahiri, Samaresh Bhattacharya, Barindra Kumar Ghosh, and Animesh Chakravorty*

Received June 18, 1986

The N,O ligands concerned are HQ = 2-R-8-quinolinol (R = H, Me) and HL = *N*-arylsalicylaldimine, *p*-$RC_6H_4N{=}CHC_6H_4OH$ (R = H, Me, OMe, CO_2Et, Cl). The trivalent complexes synthesized are MQ_3 (**3** (M = Ru) and **8** (M = Os)), RuL_3 (**4**), and $[Et_4N][OsX_2Q_2]$ (**7**, X = Cl, Br), and the quadrivalent species are $[RuL_3]PF_6$ (**5**), $[OsQ_3]ClO_4$ (**9**), and OsX_2Q_2 (**6**). Species **3** and **4** are obtained by the reaction of ligands with ruthenium trichloride and tris(acetylacetonate), respectively; **5** is electrosynthesized. The reaction of HQ with diammonium hexahaloosmate affords **6**, which on further reaction with HQ furnishes **8**. The syntheses of **7** and **9** are respectively achieved by reduction (hydrazine hydrate) of **6** and oxidation (cerium(IV)) of **8**. On the basis of IR data, doping experiments, electrochemical behavior, and steric considerations, it is concluded that the tris complexes have meridional MN_3O_3 coordination spheres while **6** and **7** have the $MX_2N_2O_2$ sphere in a trans-trans-trans geometry. All complexes display two cyclic voltammetric responses due to M(IV)/M(III) and M(III)/M(II) couples, and in the case of **8** a third couple corresponding to a higher level of oxidation is also observed. The formal potentials of the type **4** complexes linearly correlate with the Hammett constant of the R substituent. The trivalent complexes are one-electron paramagnets (idealized t_{2g}^5) and display characteristic rhombic EPR spectra. Two ligand field transitions within the three Kramers doublets have been identified in the near-IR region (<8500 cm^{-1}). The *g* components are assigned on this basis, affording values of axial (Δ) and rhombic (V) distortion parameters. The complexes generally have large distortions, and values of Δ and V span the ranges 4000-6000 and 500-2000 cm^{-1}, respectively. The RuL_3 complexes are more distorted than the RuQ_3 species.

Introduction

The study of the electronic structure and distortion of pseudooctahedral complexes of trivalent ruthenium and osmium with the help of spectroscopic techniques is of current interest.[1-3] We have been active in this area, and the present work forms part of this activity.[4,5] Successful synthesis and characterization of new complexes constitute the essential prerequisite of our studies, and electrochemical/chemical linkup of the trivalent species with congeners at higher and lower oxidation levels defines the broader framework of the program. The specific concern of this paper is the case of ruthenium and osmium chelated to bidentate N,O ligands, particularly in the tris fashion. To our knowledge this work represents the first thorough and systematic attempt to experimentally quantitate electronic distortions of the $M^{III}N_3O_3$ coordination sphere (M = Ru, Os).

Two familiar ligand types have been chosen, viz., 8-quinolinols and salicylaldimines. The coordination chemistry of the former, which affords the five-membered ring MQ (**1**) with numerous

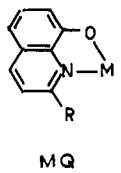

MQ

R	Q
H	Q^1
Me	Q^2

1

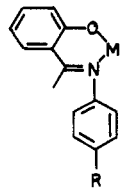

ML

R	L	R	L
H	L^1	CO_2Et	L^4
Me	L^2	Cl	L^5
OMe	L^3		

2

metal ions, has been widely investigated.[6-10] The formation of a green color by the interaction of 8-quinolinol with ruthenium(III) was reported years ago.[11] The tris chelate (RuQ^1_3)[12-14] as well as some organometallics containing Q^1 as coligand[15-17] have since been reported. Little is known about osmium complexes beyond the utilization of 8-quinolinol in a chemical analysis of the metal.[18]

Scheme I[a]

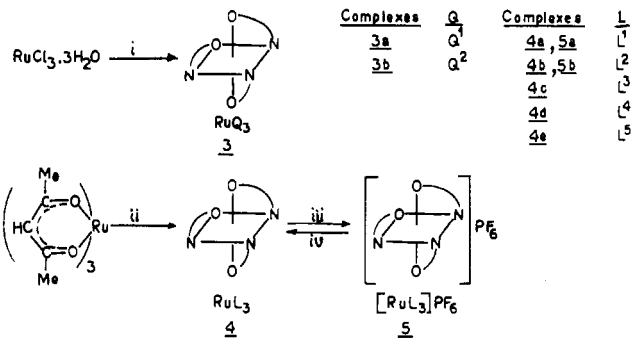

[a] Legend: (i) HQ, $MeCO_2Na$; EtOH, boil; (ii) HL; $PhCO_2Et$, boil; (iii) coulometry (0.9 V), MeCN, NH_4PF_6; (iv) coulometry (0.4 V), MeCN, NH_4PF_6.

(1) Daul, C.; Goursot, A. *Inorg. Chem.* **1985**, *24*, 3554-3558. Bernhard, P.; Stebler, A.; Ludi, A. *Inorg. Chem.* **1984**, *23*, 2151-2155.
(2) Neuenschwander, K.; Piepho, S. B.; Schatz, P. N. *J. Am. Chem. Soc.* **1985**, *107*, 7862-7869. Stebler, A.; Ammeter, J. H.; Furholz, U.; Ludi, A. *Inorg. Chem.* **1984**, *23*, 2764-2767. Hush, N. S.; Edgar, A.; Beattie, J. K. *Chem. Phys. Lett.* **1980**, *69*, 128-133.
(3) Kober, E. M.; Meyer, T. J. *Inorg. Chem.* **1983**, *22*, 1614-1616. DeSimone, R. E.; Drago, R. S. *J. Am. Chem. Soc.* **1970**, *92*, 2343-2352.
(4) Bhattacharya, S.; Ghosh, P.; Chakravorty, A. *Inorg. Chem.* **1985**, *24*, 3224-3230. Mahapatra, A. K.; Datta, S.; Goswami, S.; Mukherjee, M.; Mukherjee, A. K.; Chakravorty, A. *Inorg. Chem.* **1986**, *25*, 1715-1721.
(5) Chakravarty, A. R.; Chakravorty, A. *J. Chem. Soc., Dalton Trans.* **1982**, 615-622.
(6) Ohakaku, N.; Nakamoto, K. *Inorg. Chem.* **1971**, *10*, 798-805 and references therein.
(7) Seo, E. T.; Riechel, T. L.; Sawyer, D. T. *Inorg. Chem.* **1977**, *16*, 734-738. Isbell, A. F., Jr.; Sawyer, D. T. *Inorg. Chem.* **1971**, *10*, 2449-2457. Riechel, T. L.; Sawyer, D. T. *Inorg. Chem.* **1975**, *14*, 1869-1875.
(8) Archer, R. D.; Weber, C. J. *Inorg. Chem.* **1984**, *23*, 4158-4162. Weber, C. J.; Archer, R. D. *Inorg. Chem.* **1983**, *22*, 4149-4152.
(9) Cheng, W. *J. Coord. Chem.* **1983**, *13*, 57-62.
(10) Yamada, S.; Katayama, C.; Tanaka, J.; Tanaka, M. *Inorg. Chem.* **1984**, *23*, 253-255. Wilcox, B. E.; Heeg, M. J.; Deutsch, E. *Inorg. Chem.* **1984**, *23*, 2962-2967. Chatt, J.; Crichton, B. A. L.; Dilworth, J. R.; Dahlstrom, P.; Zubieta, J. A. *J. Chem. Soc., Dalton Trans.* **1982**, 1041-1047.
(11) Welcher, F. J. *Organic Analytical Reagents*; Van Nostrand: New York, 1947; Vol. I, p 263.
(12) Luchkina, S. A.; Sergeeva, T. P. *Russ. J. Inorg. Chem.* (*Engl. Transl.*) **1983**, *28*, 1466-1468.
(13) Domracheva, N. E.; Konstantinov, V. N.; Luchkina, S. A.; Orchinnikov, I. V. *Koord. Khim.* **1985**, *11*, 503-509; *Chem. Abstr.* **1985**, *103*, 63742j.
(14) Rodman, G. S.; Nagle, J. K. *Inorg. Chim. Acta* **1985**, *105*, 205-208.
(15) Powell, P. *J. Organomet. Chem.* **1974**, *65*, 89-92.
(16) Van Doorn, J. A.; Van Leeuween, P. W. N. M. *J. Organomet. Chem.* **1981**, *222*, 299-309.
(17) Gopinathan, S.; Deshpande, S. S.; Gopinathan, C. *Z. Anorg. Allg. Chem.* **1985**, *527*, 203-207; *Chem. Abstr.* **1986**, *104*, 27831z.

0020-1669/87/1326-4324$01.50/0

Scheme II[a]

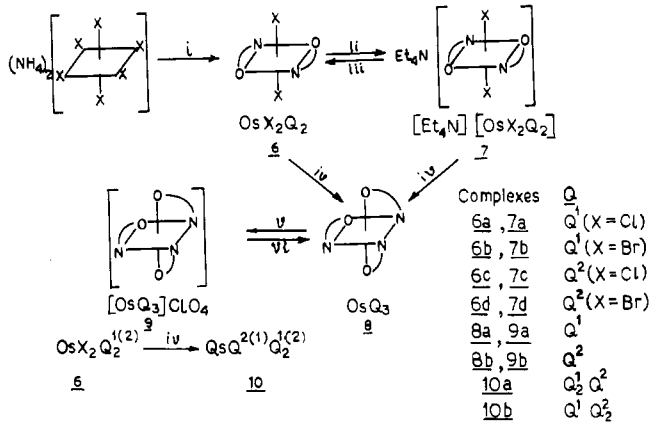

[a] Legend: (i) HQ, 2-methoxyethanol, boil; (ii) $N_2H_4 \cdot H_2O$, MeCN, Et_4NCl, stir; (iii) $Ce(SO_4)_2$, MeCN–H_2O, stir; (iv) HQ, 2-methoxyethanol–water, stir; (v) $Ce(SO_4)_2$, CH_2Cl_2–CH_3CN, $NaClO_4$, stir; (vi) $N_2H_4 \cdot H_2O$, CH_3CN, stir.

Metal salicylaldimines (six-membered chelate ring ML (**2**)) constitute one of the most studied groups in coordination chemistry.[19] Ruthenium salicylaldimines are however sparsely studied; only one tris chelate[20] and a few species of other types[21,22] are known.

Herein we report the synthesis and characterization of the meridional metal(III) tris chelates of types RuQ_3, OsQ_3, and RuL_3. Their electronic structure is probed with the help of EPR and near-IR spectroscopy. The accessibility of other (+2, +4, +5(?)) metal oxidation levels in the tris chelates is examined with the help of electrochemical techniques and in some cases by chemical synthesis. Attention is also given to OsX_2Q_2 and its reduced derivative $OsX_2Q_2^-$ (X = Cl, Br); the former appears as an intermediate in the synthesis of OsQ_3.

Results and Discussion

A. Synthesis. Two Q and five L ligands differing in R substituents were used in the present work (**1**, **2**). Specific ligands are identified with the help of a superscript as shown in **1** and **2** (e.g., when R = H, the Q ligand is called Q^1 and so on). Pure solid complexes isolated in the present work, their number designation, the routes used for their syntheses, and their gross geometries are summarized in Schemes I and II. All the reported complexes except RuQ^1_3 are new. The chelate displacement method used for the synthesis of **4** (Scheme I) was reported earlier for a related complex.[20]

The trivalent complexes RuL_3, MQ_3, and $OsX_2Q_2^-$, which constitute the main concern of this work, are uniformly one-electron paramagnets (1.9–1.7 μ_B, Table I) corresponding to a low-spin d^5 configuration. These are more or less soluble in dichloromethane and acetonitrile, affording greenish (**3**, **4**) or reddish (**7**, **8**) solutions. Complexes of type **7** are 1:1 electrolytes in acetonitrile (Λ_M (Ω^{-1} cm^2 M^{-1}): **7a**, 110; **7b**, 115; **7c**, 120; **7d**, 110), and all others are nonelectrolytes.

Among tetravalent complexes diamagnetic and nonelectrolytic **6** appeared as a serendipitous intermediate in the synthesis of **8** (the mixed tris chelates (**10**) could also be generated from **6**) and upon reduction afforded **7**. The other two tetravalent species isolated by electrochemical or chemical synthesis are **5** and **9**. Both species are 1:1 electrolytes in acetonitrile (Λ_M (Ω^{-1} cm^2 M^{-1}): **5a**, 150; **5b**, 140; **9a**, 140; **9b**, 130).

B. Electrochemical Linkup of Oxidation States. When one starts from either trivalent or tetravalent species, two cyclic voltammetric (CV) responses due to metal(IV)/metal(III) and metal(III)/metal(II) couples are seen in all cases. For **8** a third couple corresponding to a higher level of oxidation is also observed. Electrochemical data (all potentials are referenced to the SCE) are in Table II and Figure 1.

Table I. Bulk Magnetic Moments,[a] EPR g Values,[b] and Near-IR Absorption Maxima[c,d]

compd	μ_{eff}, μ_B	g_1	g_2	g_3	ν,[e] cm^{-1} (ec,[f] M^{-1} cm^{-1})
3a	1.89	2.358	2.176	1.810	g, 6250 (120)
		2.351[h]	2.164[h]	1.793[h]	
3b	1.87	2.399	2.156	1.789	g, 6340 (160)
4a	1.73	2.221	2.106	1.892	4440 (60), 6250 (110)
		2.214[i]	2.107[i]	1.892[i]	
4b	1.78	2.230	2.110	1.894	4440 (60), 6250 (100)
4c	1.70	2.225	2.109	1.895	4500 (60), 6330 (120)
4d	1.71	2.229	2.108	1.899	4500 (60), 6360 (120)
4e	1.74	2.230	2.111	1.899	4500 (60), 6340 (130)
7a	1.71	2.548	2.430	(1.0)[j]	5590 (330), 7600 (390)
7b	1.75	2.539	2.427	(1.0)[j]	5460 (240), 7490 (290)
7c	1.79	2.653	2.400	(1.1)[j]	5800 (140), 8070 (120)
7d	1.73	2.728	2.335	(1.1)[j]	5650 (110), 7840 (80)
8a	1.83	2.732	1.956	(0.7)[j]	4550 (350), 7900 (280)
8b	1.74	2.843	1.934	(0.7)[j]	4610 (260), 8100 (290)

[a] In the solid state at 298 K. [b] Unless otherwise stated, measurements were made in 1:1 dichloromethane–toluene (**3**, **7** and **8**) or 1:1 chloroform–toluene (**4**) glasses at 77 K. [c] Solvents used: **3** and **8**, CH_2Cl_2; **4**, CCl_4; **7**, MeCN. [d] For complexes of types **3** and **4** tabulated ν and ec values are obtained by Gaussian analysis (see text). [e] Band maxima. [f] Extinction coefficient. [g] Band maxima <4000 cm^{-1}. [h] In *mer*-CoQ^1_3 matrix (1%, 77 K). [i] In *mer*-CoL^1_3 matrix (1%, 77 K). [j] Calculated values (see text and Table III).

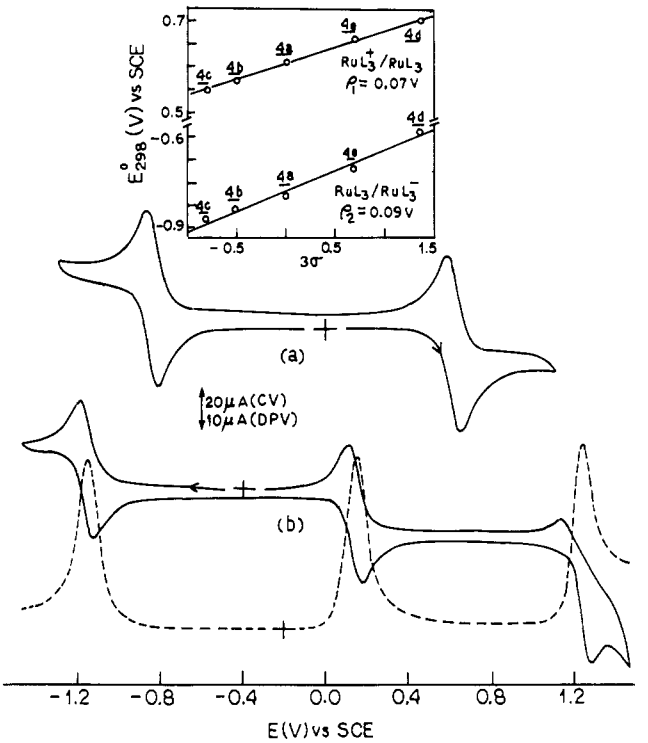

Figure 1. Voltammograms (298 K) in acetonitrile (0.1 M TEAP) at a platinum electrode: (a) CV of RuL^1_3 (**4a**), scan rate 50 mV s^{-1}; (b) CV of OsQ^2_3 (**8b**), scan rate, 50 mV s^{-1} (—) and DPV of **8b**, scan rate, 10 mV s^{-1} (---). The solute concentration in each case is $\sim 10^{-3}$ M. The inset shows least-squares plot of E°_{298} values of the couples RuL_3^+/RuL_3 and RuL_3/RuL_3^- vs. 3σ.

(18) Puri, B. K.; Goutam, M.; Kumar, A.; Wasey, A.; Hassain, M. F.; Sethi, C. L. *Chem. Scr.* **1983**, *22*, 19–21; *Chem. Abstr.* **1983**, *99*, 15715e. Wenclawiak, B.; Bickman, F. *Bunseki Kagaku* **1984**, *33*, E67–E72; *Chem. Abstr.* **1984**, *100*, 131573v.
(19) It is unfortunate that no comprehensive recent review on metal salicylaldimines is available. A dated but exhaustive review is: Holm, R. H.; Everett, G. W., Jr.; Chakravorty, A. *Prog. Inorg. Chem.* **1966**, *7*, 83–214.
(20) Finney, K. S.; Everett, G. W., Jr. *Inorg. Chim. Acta* **1974**, *11*, 185–188.
(21) Calderazzo, F.; Floriani, C.; Henzi, R.; L'Eplattenier, F. *J. Chem. Soc. A* **1969**, 1378–1386.
(22) Thornback, J. R.; Wilkinson, G. *J. Chem. Soc., Dalton Trans.* **1978**, 110–115 and references therein. Murray, K. S.; van den Bergen, A. M.; West, B. O. *Aust. J. Chem.* **1978**, *31*, 203–207.

Table II. Electrochemical Data[a-d] at 298 K

compd	$E°_{298}$, V (ΔE_p, mV) M(IV)/M(III)	$E°_{298}$, V (ΔE_p, mV) M(III)/M(II)	compd	$E°_{298}$, V (ΔE_p, mV) M(IV)/M(III)	$E°_{298}$, V (ΔE_p, mV) M(III)/M(II)
3a	0.66[e] (130)	−0.70[f] (70)	**7a**	0.02[k] (70)	−1.45[l] (80)
3b	0.59 (110)	−0.82 (70)	**7b**	0.07 (80)	−1.36 (70)
4a	0.61[g] (60)	−0.83[h] (60)	**7c**	−0.12 (80)	−1.67 (90)
4b	0.57 (60)	−0.86 (80)	**7d**	−0.03 (70)	−1.52 (80)
4c	0.55 (60)	−0.88 (60)	**8a**[o]	0.25[m] (60)	−0.96[n] (60)
4d	0.70[i] (60)	−0.69[j] (60)	**8b**[o]	0.14 (60)	−1.16 (60)
4e	0.66 (70)	−0.77 (70)	**10a**[o]	0.19 (60)	−1.08 (60)
			10b[o]	0.16 (60)	−1.13 (60)

[a] Meaning and units of symbols are the same as in the text. [b] Conditions: solvent, MeCN; supporting electrolyte, TEAP (0.1 M); working electrode, platinum; reference electrode, SCE; solute concentration, $\sim 10^{-3}$ M. [c] Cyclic voltammetric data: scan rate 50 mV s^{-1}. [d] Constant-potential coulometry (oxidation done at potential $E°_{298}$ + 200 mV and reduction at $E°_{298}$ − 200 mV) was performed in selected cases: $n = Q/Q'$ where Q' is the calculated coulomb count for 1e transfer and Q is the coulomb count found after exhaustive electrolysis of 0.01 mmol of solute. [e] A reliable n value could not be determined due to continuous accumulation of coulombs. [f] n = 1.02. [g] n = 0.95. [h] n = 0.98. [i] n = 0.90. [j] n = 0.97. [k] n = 1.03. [l] n = 0.97. [m] n = 1.01. [n] n = 0.98. [o] $E°_{298}$ (ΔE_p) values of a third response are as follows: **8a**, 1.26 (160); **8b**, 1.20 (160); **10a**, 1.23 (130); **10b**, 1.21 (130).

Complexes **4** and **5** afford the same CV responses. The nearly reversible couples 1 and 2 with peak-to-peak separations (ΔE_p)

$$RuL_3^+ + e^- \rightleftharpoons RuL_3 \quad (1)$$

$$RuL_3 + e^- \rightleftharpoons RuL_3^- \quad (2)$$

of 60–80 mV are observed. The formal potentials ($E°_{298}$) of the couples increase systematically with increasing electron-withdrawing character of R. The plot of $E°_{298}$ vs 3σ is linear for both couples (Figure 1) with ρ_1 = 0.07 V and ρ_2 = 0.09 V (σ, Hammett constant of R; ρ_i, reaction constant of couple i).[23] The one-electron stoichiometry of each of the couples was confirmed coulometrically. Coulometrically produced solutions of RuL_3^- are dark violet (absorption maximum at $\sim$540 nm) and quite sensitive to air. Frozen solutions did not afford any EPR signal, suggesting a spin-paired t_{2g}^6 configuration. Neither RuL_3^- nor the electrogenerated bivalent species of the other complexes studied in this work have been isolated in a pure form as salts.

In the case of **3**, the RuQ_3^+/RuQ_3 and RuQ_3/RuQ_3^- couples are observed and their formal potentials lie close to those of couples 1 and 2, respectively. The observation of the RuQ_3^+/RuQ_3 response is complicated by the formation of a dark yellow coating of presumably polymeric species[24] on the working electrode upon oxidation. The response is however still observable during the first CV cycle. Dichloromethane is a better solvent for this observation even though ΔE_p values are large. The formation of the yellow coating has vitiated quantitation of the coulometric oxidation of RuQ_3 to RuQ_3^+ and possible isolation of the latter. The yellow species is under further scrutiny.

Both CV and differential pulse voltammetry (DPV) were used to study OsQ_3 (Figure 1). The OsQ_3^+/OsQ_3 formal potential is substantially less than the RuQ_3^+/RuQ_3 potential, and a similar relationship holds between the MQ_3/MQ_3^- potentials. This reflects the better stability of the higher oxidation states in the heavier metal. Indeed, OsQ_3 displays a third response, OsQ_3^{2+}/OsQ_3^+, near 1.2 V in which the OsQ_3^{2+} species may have pentavalent osmium. The transformation $OsQ_3^+ \rightarrow OsQ_3^{2+}$ is attended with yellow deposition as in the case of $RuQ_3 \rightarrow RuQ_3^+$ oxidation. In addition to making the OsQ_3^{2+}/OsQ_3^+ response distorted, this has made isolation and characterization of OsQ_3^{2+} inaccessible. Interestingly, the formal potentials of the three OsQ_3 couples compare well with those[25] of OsD_3^{2+}/OsD_3^+, OsD_3^+/OsD_3, and OsD_3/OsD_3^- (D = *N*,*N*-diethyldithiocarbamate).

The formal potentials of Q^1 and Q^2 complexes reflect the electron-donating character of the methyl groups: compare the tetrad OsQ^1_3, $OsQ^1_2Q^2$, $OsQ^1Q^2_2$, and OsQ^2_3. Complexes of type **7** are also electroactive, affording well-behaved osmium(IV)/osmium(III) and osmium(III)/osmium(II) couples. An ill-defined response is also observed above 1.2 V. This has not been examined in detail.

C. Molecular Geometry. The OsX_2Q_2 and $OsX_2Q_2^-$ complexes are assigned a trans-trans-trans geometry (**6**, **7**). The X = Cl complexes display a sharp single OsCl stretch (absent in X = Br complexes) in accord with the trans configuration of the $OsCl_2$ fragment (ν_{OsCl} (cm^{-1}): **6a**, 330; **6c**, 335; **7a**, 305; **7c**, 310 (the decrease in going from **6** to **7** is due to a decrease in metal oxidation level)). Scale models constructed with known dimensions[10] of coordinated Q^1 and Q^2 demonstrate that the geometry of the grossly planar OsQ_2 fragment must be trans at least for the Q^2 complexes, where the cis geometry is found to involve very severe crowding of the two methyl groups. Since the Q^1 and Q^2 complexes are very similar in their properties and they are formed with equal ease, it is inferred that they have the same stereochemistry (**6**, **7**).

The question of isomeric structures of RuQ^1_3 has been raised but not resolved.[14] Each of the RuQ_3 and OsQ_3 complexes was obtained by us in only one isomeric form. Isomeric homogeneity was checked by careful chromatography on silica gel and alumina. The complex CoQ^1_3 is known[9] in both meridional and facial forms—the former being the major product. Except for a small displacement of frequencies there is a one-to-one correspondence of bands in the IR spectra (1600–500 cm^{-1}) of RuQ^1_3 and pure meridional CoQ^1_3. The same relationship holds between the IR spectra of OsQ^1_3 and RuQ^1_3. Further, RuQ^1_3 freely grows in the lattice of meridional CoQ^1_3 and the EPR spectrum of such a doped lattice is considered later in this work. On the basis of this evidence it is concluded that RuQ^1_3 and OsQ^1_3 and by inference RuQ^2_3 and OsQ^2_3 have meridional geometry (**3**, **8**). The conversion **6** → **8** involves stereochemical rearrangement, and it is significant that the reaction is very slow. Cobalt(III) salicylaldimines, CoL_3, occur exclusively in the sterically favorable meridional form.[26] The stereochemistry of RuL_3 was correlated with that of CoL_3 by using IR and doped-lattice EPR (see below) data. Thus, like RuQ_3, RuL_3 has meridional geometry (**4**). This geometry has also been assigned to a related tris chelate on the basis of CD spectra and chromatographic behavior.[20]

The IR spectrum of $[RuL_3]PF_6$ is virtually superposable on that of RuL_3 except for the strong PF_6^- band near 840 cm^{-1}. This observation and the reversibility of the RuL_3^+/RuL_3 couple show that the oxidation of RuL_3 is stereoretentive. This is reasonable since the same steric factors that make RuL_3 meridional will be even more strongly operative in RuL_3^+ due to the smaller size of the oxidized metal ion. A similar relation must exist between OsQ_3 and OsQ_3^+.

D. Distortion Parameters of Trivalent Species. The meridional tris chelates MQ_3 and RuL_3 have no symmetry (C_1), and the anion $OsX_2Q_2^-$ can at best have C_{2h} symmetry. Rhombic EPR spectra are therefore expected for all the species. This is indeed found in practice. EPR spectra were measured in chloroform/toluene or dichloromethane/toluene glasses or in a polycrystalline doped cobalt(III) lattice. Data are in Table I and Figure 2. The ruthenium(III) species uniformly display three resonances characterizing a rhombic structure. The corresponding g components are designated g_1, g_2, and g_3 in order of decreasing magnitudes. Only two resonances (g_1 and g_2) are observable for the osmium(III) chelates, and we shall comment on g_3 later.

The theory of the EPR spectra of distorted-octahedral low-spin d^5 (idealized t_{2g}^5; ground term $^2T_{2g}$) complexes are documented in the literature.[1-4,27-29] Only the essential features of relevance

(23) Mukherjee, R. N.; Rajan, O. A.; Chakravorty, A. *Inorg. Chem.* **1982**, *21*, 785–790.
(24) Pham, M. C.; Dubois, J. E.; Lacaze, P. C. *J. Electrochem. Soc.* **1983**, *130*, 346–351.
(25) Wheeler, S. H.; Pignolet, L. H. *Inorg. Chem.* **1980**, *19*, 972–979.
(26) Chakravorty, A.; Holm, R. H. *Inorg. Chem.* **1964**, *3*, 1521–1524.
(27) Griffith, J. S. *The Theory of Transition Metal Ions*; Cambridge University Press: London, 1961; p 364. Bleany, B.; O'Brien, M. C. M. *Proc. Phys. Soc., London, Sect. B* **1956**, *69*, 1216–1230.

Table III. Assignments of g Values and Values of Parameters[a]

compd	soln no.	g_x	g_y	g_z	p	q	r	k	Δ/λ	V/λ	ϵ_1/λ	ϵ_2/λ
3a	1	−2.358	−2.176	1.810	0.188	0.981	0.036	0.651	4.237	−1.844	3.432	5.446
	2	−2.358	−2.176	−1.810	0.785	0.619	0.018	1.091	0.162	−0.071	1.450	1.564
3b	1	−2.399	−2.156	1.789	0.196	0.979	0.046	0.660	4.153	−2.266	3.170	5.562
	2	−2.399	−2.156	−1.789	0.783	0.622	0.024	1.092	0.174	−0.096	1.445	1.572
4a	1	−2.221	−2.106	1.892	0.145	0.989	0.028	0.512	5.460	2.388	4.350	6.881
	2	−2.221	−2.106	−1.892	0.798	0.603	0.011	1.057	0.098	−0.044	1.468	1.537
4b	1	−2.230	−2.110	1.894	0.143	0.989	0.029	0.532	5.549	2.508	4.380	7.024
	2	−2.230	−2.110	−1.894	0.798	0.603	0.012	1.060	0.100	−0.046	1.467	1.538
4c	1	−2.225	−2.109	1.895	0.142	0.989	0.029	0.525	5.555	−2.465	4.406	7.010
	2	−2.225	−2.109	−1.895	0.798	0.603	0.012	1.059	0.098	−0.045	1.468	1.537
4d	1	−2.229	−2.108	1.899	0.139	0.990	0.029	0.537	5.698	−2.652	4.457	7.238
	2	−2.229	−2.108	−1.899	0.798	0.603	0.012	1.061	0.098	−0.047	1.468	1.537
4e	1	−2.230	−2.111	1.899	0.140	0.990	0.029	0.541	5.678	−2.574	4.474	7.182
	2	−2.230	−2.111	−1.899	0.798	0.603	0.012	1.062	0.098	−0.046	1.468	1.538
7a	1	−2.548	−2.430	(1.0)	0.424	0.905	0.016	0.781	1.684	−0.189	1.834	2.526
7b	1	−2.539	−2.427	(1.0)	0.424	0.905	0.015	0.776	1.681	−0.180	1.833	2.523
7c	1	−2.153	−2.400	(1.0)	0.420	0.907	0.033	0.818	1.711	−0.404	1.819	2.589
7d	1	−2.728	−2.335	(1.0)	0.419	0.906	0.052	0.826	1.741	−0.634	1.783	2.679
8a	1	−2.732	−1.956	(0.7)	0.485	0.868	0.107	0.700	1.485	−1.046	1.512	2.643
8b	1	−2.843	−1.934	(0.7)	0.480	0.869	0.121	0.745	1.546	−1.231	1.490	2.773

[a] Symbols have the same meaning as in the text.

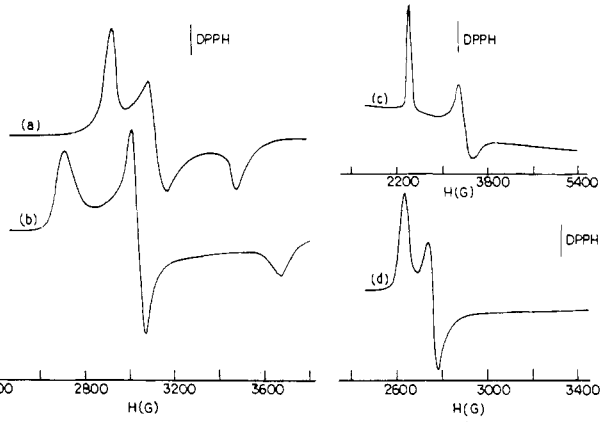

Figure 2. EPR spectra (X-band) at 77 K: (a) RuL^1_3 (**4a**) doped in CoL^1_3; (b) RuQ^1_3 (**3a**) doped in CoQ^1_3; (c) OsQ^1_3 (**8a**) in a 1:1 acetonitrile–toluene glass; (d) $[Et_4N][OsCl_2Q^1_2]$ (**7a**) in a 1:1 acetonitrile–toluene glass.

to the present work will be stated here. Quite generally the net distortion of pseudooctahedral species can be expressed as the sum of axial (Δ) and rhombic (V) components. The axial distortion is appropriately considered as tetragonal and trigonal for **7** and the tris chelates, respectively. The t_2 orbital consists of the components t_2^0, t_2^+, and t_2^-.[30,31] Axial distortion partly removes t_2 degeneracy, placing t_2^0 above t_2^+, t_2^- by Δ. The rhombic components split t_2^- from t_2^+ by V. The components T_2^0, T_2^+, and T_2^- of the T_2 term (spin multiplicity not shown) undergo corresponding splittings.[32] Under the influence of spin–orbit coupling (λ) the components mix, affording three Kramers doublets. The ground doublet is of the form given in eq 3. The

$$\varphi_i = p|T_2^+\rangle + q|\bar{T}_2^0\rangle + r|T_2^-\rangle$$
$$\varphi_{ii} = p|\bar{T}_2^-\rangle + q|T_2^0\rangle + r|\bar{T}_2^+\rangle \quad (3)$$

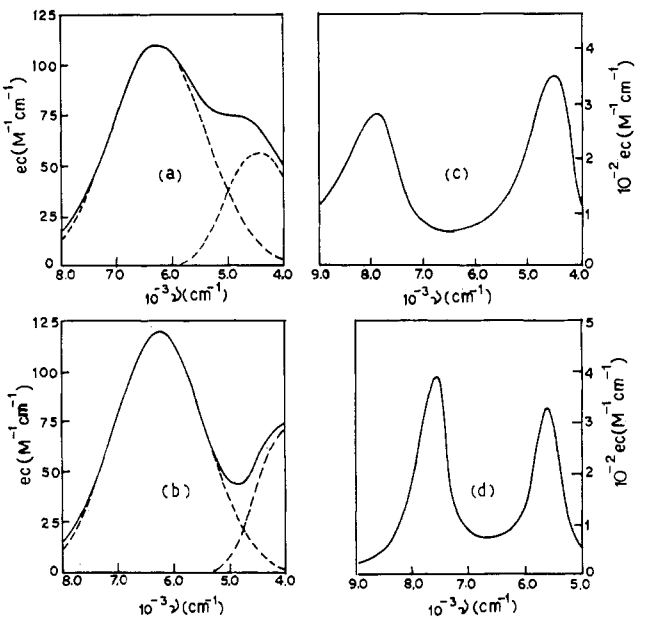

Figure 3. Near-IR spectra: (a) RuL^1_3 (**4a**) in CCl_4; (b) RuQ^1_3 (**3a**) in CH_2Cl_2; (c) OsQ^1_3 (**8a**) in CH_2Cl_2; (d) $[Et_4N][OsCl_2Q^1_2]$ (**7a**) in CH_3CN.

EPR g tensors arising from this doublet can be expressed as in eq 4–6, where k is the orbital reduction factor.[33] Two crystal

$$g_x = 2[-2pr - q^2 - 2^{1/2}kq(p + r)] \quad (4)$$
$$g_y = 2[2pr - q^2 - 2^{1/2}kq(p - r)] \quad (5)$$
$$g_z = 2[-p^2 + q^2 - r^2 - k(p^2 - r^2)] \quad (6)$$

field transitions (energies ϵ_1 and ϵ_2, $\epsilon_1 < \epsilon_2$) should arise due to optical transitions from ground to upper doublets. The availability of experimental ϵ_1 and ϵ_2 values is crucial for choosing the correct solution through comparison with computed values. The corresponding values of Δ, V, and k as well as of p, q, and r are then easily extracted. This approach is utilized in the present work. The ϵ_1 and ϵ_2 transitions have been systematically identified for all the complexes (Figure 3, Table I).

Without placement of any constraint on ϵ_1 and ϵ_2 values two alternative solutions differing in the sign of g_z occur in the cases

(28) Hill, N. J. *J. Chem. Soc., Faraday Trans. 2* **1972**, *68*, 427–434.
(29) Bhattacharya, S.; Chakravorty, A. *Proc.—Indian Acad. Sci., Chem. Sci.* **1985**, *95*, 159–167.
(30) Under tetragonal quantization the components are $t_2^0 = xy$, $t_2^+ = xz$, and $t_2^- = yz$, and under trigonal quantization they are $t_2^0 = z^2$, $t_2^+ = (2/3)^{1/2}(x^2 - y^2) - (1/3)^{1/2}xz$, and $t_2^- = (2/3)^{1/2}xy + (1/3)^{1/2}yz$.
(31) Ballhausen, C. J. *Introduction to Ligand Field Theory*; McGraw-Hill: New York, 1962; p 99–106.
(32) In T_2^0, T_2^+, and T_2^- the unpaired electron is respectively in the t_2^0, t_2^+, and t_2^- orbitals. In tetragonal geometry t_2^0 and t_2^+, t_2^- span b and e representations (T_2^0, B; T_2^+ and T_2^-, E) while in the trigonal case the corresponding representations are a and e (A, E). In rhombic geometry e (E) splits into orbital singlets of representations appropriate for the particular symmetry. In order to avoid confusion of multiple representation symbols, the t_2 (T_2) labels with 0, +, and − superscripts are used in this work.
(33) Changing the signs of any two of the equations among eq 4–6 leaves the physical results unaffected. The chosen signs in eq 4–6 afford identical values of g_x and g_y in the axial situation ($r = 0$) as in our previous work.[4,29]

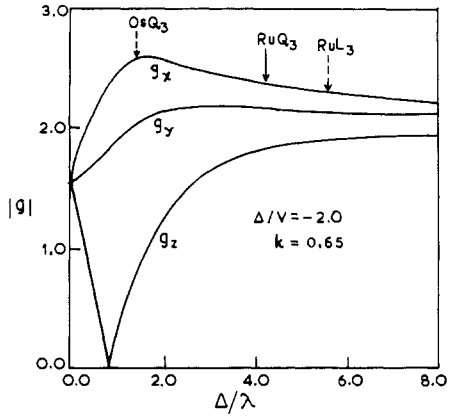

Figure 4. Variation of g components as a function of Δ/λ.

of RuL_3 and RuQ_3 (Table III). This ambiguity cannot be resolved by EPR experiments, which can afford only the magnitude of g components. The two solutions however differ widely in the values of the distortion parameters as well as of ϵ_1 and ϵ_2. Distortion is much higher in solution 1.

We consider RuL_3 first. The spin–orbit coupling constant of *complexed* ruthenium(III) can be taken[1-4] as $\sim$1000 cm^{-1}. From Table III we observe that $\epsilon_1 \approx 4500$, $\epsilon_2 \approx 7000$ cm^{-1} (solution 1) and $\epsilon_1 \approx \epsilon_2 \approx 1500$ cm^{-1} (solution 2). As stated earlier, the IR spectra of RuL_3 and CoL_3 display one-to-one correspondence and no new bands occur at $\sim$1500 cm^{-1} in RuL_3. On the other hand, two overlapping bands occur in the near-IR spectra of RuL_3 taken in CCl_4 solution (Figure 3) and such bands are absent in CoL_3. The observed feature of RuL_3 can be resolved into two Gaussian components (Table I) at $\sim$4500 and $\sim$6300 cm^{-1} with molar extinction coefficients in the range 50–130 M^{-1} cm^{-1}.[34] Considering the inherent approximations in the theory used, the observed ϵ_1 and ϵ_2 values are in excellent agreement with solution 1. The ground state so defined is nearly 98% T_2^0 in character ($q \approx 0.99$).

In qualitative terms RuQ_3 is entirely analogous to RuL_3 with two possible solutions having opposite signs of g_z and differing widely in the values of ϵ_1 and ϵ_2 (Table III). Solution 2 can be discarded on grounds similar to those used in the case of RuL_3. Solution 1 predicts ϵ_1 and ϵ_2 transitions at $\sim$3200 and $\sim$5500 cm^{-1}, respectively. The latter transition is clearly observed at $\sim$6300 cm^{-1}, and the former transition is discernible in the rising absorption at lower energies (Figure 3).[35] The near-IR data therefore unequivocally support the high-distortion solution 1 for RuQ_3. The UV–vis spectrum of RuQ^1_3 has been reported in a recent study, but the near-IR region was not examined.[14]

The EPR spectra of RuQ^1_3 were reported earlier in frozen chloroform solution and in liquid-crystal media.[12,13] The spectra compare favorably with ours. No attempt was made, however, to compute and experimentally identify the ϵ_1 and ϵ_2 transitions, and a low-distortion solution was chosen arbitrarily.[13] The present work firmly refutes this choice.

For OsQ_3 only two EPR signals are observed. The nature and shape of the spectra (Figure 2) strongly suggest that these correspond to the g_1 and g_2 transitions of RuQ_3. The third OsQ_3 resonance could not be experimentally identified.[36] Fortunately the ϵ_1 and ϵ_2 optical transitions are observable in the near-IR region (Figure 3, Table I). We estimate g_3 and derive an internally consistent set of parameters as follows.

In Figure 4 we display the computed variations of g_x, g_y, and g_z with Δ/λ. The parameters Δ, Δ/V, and k corresponding to

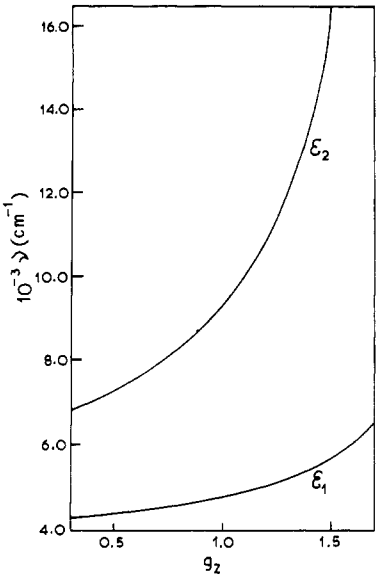

Figure 5. Variation of ϵ_1 and ϵ_2 as a function of g_z (the values of g_x and g_y are fixed at 2.732 and 1.956, respectively).

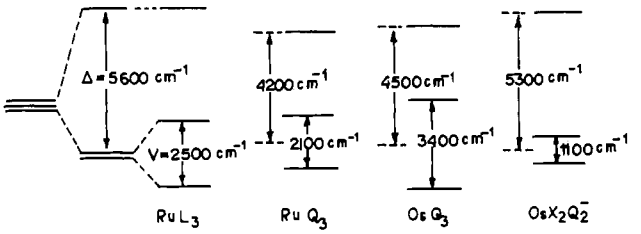

Figure 6. Average axial and rhombic splitting parameters for four groups of complexes.

solution 1 are initially assumed to be transferable from RuQ_3 and OsQ_3. Taking λ for osmium(III)[3,28,37,38] as 3000 cm^{-1} and setting $\Delta = 4200$ cm^{-1}, we have $\Delta/\lambda = 1.4$. The three g values corresponding to the OsQ_3 position of Figure 4 are $g_x \approx 2.6$, $g_y \approx 2.0$, and $g_z \approx 0.7$. The agreement of the g_x and g_y values with experimental g_1 (2.73, 2.84) and g_2 (1.96, 1.93) values is fair. It is therefore appropriate to take 0.7 as a fair estimated value of g_3. This parameter was then varied in steps around 0.7 until the best fit with experimental ϵ_1 and ϵ_2 values was achieved. The predicted variation of ϵ_1 and ϵ_2 as a function of g_z is shown in Figure 5. Fortuitously the best-fit g_z value equaled the initial estimated value of 0.7.[39] The observed ($\sim$4500 and $\sim$8000 cm^{-1}) and calculated ($\sim$4500 and $\sim$8100 cm^{-1}, Table III) ϵ_1 and ϵ_2 values matched well. Since g_3 is used as a variable parameter, the near-exactness of the fit does not have any special significance. The important point is that a good fit is achievable.

Like OsQ_3, $OsX_2Q_2^-$ also shows two EPR resonances and two near-IR bands (Figures 2 and 3). Since the ruthenium(III) analogue is unavailable here for comparison, the value of g_3 giving the best fit to the observed ϵ_1 and ϵ_2 values was generated by systematic computation. The two observed g components were taken as g_1 and g_2, and g_3 was varied in increments of 0.1 in the range 1.9–0.2. The best fit with experimental ϵ_1 and ϵ_2 values occurs at $g_3 = 1.0$ (Table III). A second solution corresponding to $g_x = -g_1 = -g_2$, and $g_z = -g_3$ exists, but this corresponds to unacceptably small values of ϵ_1/λ and ϵ_2/λ (e.g., 1.41 and 1.72 in the case of $Et_4N[OsCl_2Q^1_2]$).

There are variations in the computed distortion parameters (Table III) among members of each group. The substituted (R $\neq$ H) complexes appear to be more distorted than the parent

(34) Barker, B. E.; Fox, M. F. *Chem. Soc. Rev.* **1980**, *9*, 143–184.
(35) Carbon tetrachloride is the ideal solvent for near-IR studies. However, due to solubility reasons dichloromethane had to be used as the solvent for RuQ_3.
(36) Our own EPR setup scans the field range 0–6000 G. Experiments were also performed elsewhere in the range 0–10 000 G. The inability to observe an expected resonance in osmium compounds is documented in other cases.[3]
(37) Sakaki, S.; Hagiwara, N.; Yanase, Y.; Ohyoshi, A. *J. Phys. Chem.* **1979**, *82*, 1917–1920.
(38) Hudson, A.; Kennedy, M. J. *J. Chem. Soc. A* **1969**, 1116–1120.
(39) It is meaningless to express g_z to higher decimal places since ϵ_1 and ϵ_2 are not that sensitive to variation of g_z (see Figure 5).

species (R = H). In particular, the Q^2 complexes systematically display rhombic distortion higher than that of the Q^1 complexes. Significantly, in the former complexes the Me groups lie close to the coordination sphere. The average orbital splittings for each of the four groups of compounds considered above are shown in Figure 6. The low point group symmetry of the complexes finds genuine expression in their electronic structure in the form of a large anisotropy of bonding that is tantamount to the observed large distortions. The sizable axial splitting and relatively small rhombic distortion of **7** are similar to those in some $RuX_2N_2O_2$ species.[5] Interestingly, even though RuL_3 is more distorted than RuQ_3, the spread of g values is less in the former. This can be understood with reference to Figure 4. At very small values of Δ, the g components fan out rapidly with an increase in Δ, but when Δ is large, the spread actually decreases as Δ becomes larger. The approximate (since the k and Δ/V values of RuL_3 are different from those of Figure 4) location of RuL_3 is indicated in Figure 4. Quantitative rationalization of the distortion parameters of the various complexes in terms of bonding would require major computational efforts,[40] which is beyond the scope of the present work.

E. Concluding Remarks. The synthesis of groups of meridional tris chelates of type RuQ_3, RuL_3, and OsQ_3 representing the low-spin d^5 MN_3O_3 coordination sphere has been achieved. Also synthesized is the trans-trans-trans $OsX_2N_2O_2$ sphere in the form of $OsX_2Q_2^-$ (X = Cl, Br). The low molecular symmetry of the complexes is reflected in their rhombic EPR spectra. The extent of distortion from idealized O_h symmetry has been ascertained in terms of axial (Δ) and rhombic (V) components. The distortions are large enough to make the two ligand field transitions (ϵ_1, ϵ_2) among the three Kramers doublets observable in the near-IR region. Probably for the same reason the band intensities are also relatively large (50–400 M^{-1} cm^{-1}). The availability of ϵ_1 and ϵ_2 values has led to quantitation of Δ and V with the help of observed g values. In the case of the osmium complexes, where the experimental g_3 values are missing, the ϵ_1 and ϵ_2 data are used to estimate g_3 and to compute an internally consistent set of parameters. The values of k fall in the range 0.5–0.8. Ideally, k should be a measure of covalency, but as determined by the present type of analysis, it acts as a sink for unaccounted effects.[27,41] Literature values of k span the range 0.4–1.2.[1-5,27,37,38,41] The present work demonstrates that relatively low k values are not necessarily a feature of sulfur coordination.[41]

The stereoretentive oxidation of the trivalent chelates affords the EPR-inactive quadrivalent species $[RuL_3]PF_6$, $[OsQ_3]ClO_4$, and OsX_2Q_2. The oxidation states +2 and +4 can be electrochemically interlinked in solution to the +3 state in all cases. In course of this work we synthesized other 8-quinolinol species that have not been considered above. One such complex is red-violet $[Ru(bpy)_2Q^1]ClO_4$ (**11**),[42] formed by the reaction of $Ru(bpy)_2Cl_2$ with HQ^1 in ethanol in the presence of $AgClO_4$ (bpy = 2,2′-bipyridine). The dramatic difference in the relative abilities of bpy and Q^1 in stabilizing bivalent and trivalent ruthenium is reflected in a shift of ~+1.2 V in the ruthenium(III)/ruthenium(II) formal potential in going from **3** to **11** ($E°_{298}$ = 0.48V). Since bpy has two pyridine donors and Q^- has one pyridine and one phenolate donor, this result heavily underlines the strong affinity of phenolic oxygen for trivalent ruthenium (and by inference osmium). This affinity evidently extends to the tetravalent state as well.

Experimental Section

Materials. Ruthenium trichloride received from Arora-Matthey, Calcutta, India, was converted to $RuCl_3·3H_2O$ by repeated evaporation to dryness with concentrated hydrochloric acid.[43] Osmium tetraoxide also obtained from the same source was reacted with concentrated HX to afford $(NH_4)_2OsX_6$ (X = Cl, Br).[44] The complexes CoQ^1_3 and CoL^1_3 were prepared by the reported procedures.[9,26] All other chemicals (HQ ligands, salicylaldehyde, para-substituted anilines, CH_3CO_2Na, $N_2H_4·H_2O$, $Ce(SO_4)_2·4H_2O$, Et_4NCl, NH_4PF_6) and organic solvents (benzene, toluene, chloroform, 2-methoxyethanol, ethyl benzoate, ethanol) used in syntheses were reagent grade commercial materials. Silica gel (60–120 mesh) used for chromatography was of BDH make. For spectroscopic/electrochemical studies commercial solvents were purified as follows. Acetonitrile was treated with CaH_2 (overnight) followed by successive distillations over $LiCO_3$–$KMnO_4$ and P_4O_{10}.[45,46] Dichloromethane was purified with the help of $NaHCO_3$ and anhydrous $CaCl_2$ while carbon tetrachloride required successive treatments with KOH, H_2SO_4, H_2O, and anhydrous $CaCl_2$.[47] The solvents were stored over molecular sieves (4 Å). Commercial tetraethylammonium bromide was converted to pure tetraethylammonium perchlorate (TEAP) by following an available procedure.[45] Dinitrogen gas was purified by successively bubbling it through alkaline dithionite and concentrated sulfuric acid.

Measurements. Near-IR spectra were recorded by using a Hitachi 330 spectrophotometer fitted with a thermostated cell compartment. Gaussian analyses of bands where required were performed as before.[4] Infrared (4000–300 cm^{-1}) spectra were taken on a Perkin-Elmer 783 spectrophotometer. Solution electrical conductivity was measured by using a Philips PR 9500 bridge with solute concentration of $\sim 10^{-3}$ M. Magnetic susceptibilities were measured with the help of a PAR 155 vibrating-sample magnetometer fitted with a Walker Scientific L75FBAL magnet. Electrochemical measurements were done by using the PAR model 370-4 electrochemistry system incorporating the following components: 174A, polarographic analyzer; 175, universal programmer; RE0074, XY recorder; 173, potentiostat; 179, digital coulometer; 377, cell system. All experiments were performed under dinitrogen atmospheres. A planar Beckman 39273 platinum-inlay working electrode, a platinum-wire auxiliary electrode, and an aqueous saturated calomel reference electrode (SCE) were used in the three-electrode configuration. A platinum-wire-gauze working electrode were used in coulometric experiments. All electrochemical data were collected at 298 K and are uncorrected for junction potentials. EPR measurements were made with a Varian 109C E-line X-band spectrometer fitter with a quartz Dewar for measurements at 77 K (liquid dinitrogen). All spectra were calibrated with the help of DPPH (g = 2.0037). Microanalyses (C, H, N) were done by using a Perkin-Elmer 240C elemental analyzer.

The following σ values[48] for para substituents were used: H, 0.00; Me, −0.17; OMe, −0.27; CO_2Et, +0.45; Cl, +0.23.

Treatment of EPR Data. The five-electron states T_2^0, T_2^+, and T_2^- arising from population of one-electron t_2 functions split into three Kramers doublets represented by the two identical matrices in eq 7. The

		$\lvert T_2^-\rangle$ $\lvert \bar{T}_2^+\rangle$	$\lvert \bar{T}_2^0\rangle$ $\lvert T_2^0\rangle$	$\lvert T_2^+\rangle$ $\lvert \bar{T}_2^-\rangle$
$\lvert T_2^-\rangle$	$\lvert \bar{T}_2^+\rangle$	$\lambda/2$	0	$V/2$
$\lvert \bar{T}_2^0\rangle$	$\lvert T_2^0\rangle$	0	$-\Delta$	$-\lambda/2^{1/2}$
$\lvert T_2^+\rangle$	$\lvert \bar{T}_2^-\rangle$	$V/2$	$-\lambda/2^{1/2}$	$-\lambda/2$

(7)

EPR experiment affords only the magnitude of the g values but not their signs. Their correspondence to g_x, g_y, and g_z is also unknown. Each correspondence can in principle afford a set of values for p, q, r, and k in terms of eq 4–6 and the normalization equation $p^2 + q^2 + r^2 = 1$. Meaningful solutions can be sorted out by putting limits on acceptable k values such as $0 > k > 1.5$ used in the present analysis. This left only the two solutions of Table III as possibilities. The p, q, r, and k values furnish Δ, V, and the energy of the ground Kramers doublet, and diagonalization of eq 7 affords ϵ_1 and ϵ_2. Further details can be found elsewhere.[4,29] It is to be noted that when g_1, g_2, and g_3 are presented in slots of g_x, g_y, and g_z having fixed signs, a set of six solutions arise that are entirely equivalent physically.[28] These solutions are characterized by the same k, ϵ_1, and ϵ_2 values and the energy splitting diagram of the type shown in Figure 6. This permutation merely changes the names of axes and hence of orbitals. Our solution 1 (Table III) corresponds to the one-electron orbital order $t_2^0 > t_2^+ > t_2^-$.

Figure 4 was constructed in the following way. With Δ/V and k kept invariant, Δ/λ was varied in intervals of 0.2. For each value p, q, and r were computed by solving secular equations corresponding to the matrix

(40) Recently a multiple-scattering Xα MO calculation by Daul et al.[1] has helped to rationalize the trigonal splitting (~2500 cm^{-1}) of $Ru(H_2O)_6^{3+}$ (in alum) in terms of anisotropic interactions of oxygen lone pairs with t_2 orbitals.
(41) DeSimone, R. E. *J. Am. Chem. Soc.* **1973**, *95*, 6238–6244.
(42) Anal. Calcd for $RuC_{29}H_{22}N_5O_5Cl$: C, 53.00; H, 3.35; N, 10.66. Found: C, 53.20; H, 3.31; N, 10.57.
(43) Chakravarty, A. R.; Chakravorty, A. *Inorg. Chem.* **1981**, *20*, 275–278.
(44) Dwyer, F. P.; Hogarth, J. W. *Inorg. Synth.* **1957**, *5*, 204–209.
(45) Sawyer, D. T.; Roberts, J. L., Jr. *Experimental Electrochemistry for Chemists*, Wiley: New York, 1974; pp 167–215.
(46) Walter, M.; Ramaley, L. *Anal. Chem.* **1973**, *45*, 165–166.
(47) Vogel, A. I. *Practical Organic Chemistry*, 3rd ed.; ELBS and Longman Group: Harlow, England, 1965; Chapter 2, pp 176–177.
(48) Hammett, L. P. *Physical Organic Chemistry*, 2nd ed.; McGraw-Hill: New York, 1970.

of eq 7. The values of g_x, g_y, and g_z were then computed from eq 4–6.

Preparation of Complexes. Tris(8-quinolinolato)ruthenium(III), RuQ^1_3 (3a). The synthesis of this complex from NaQ^1 and $RuCl_3 \cdot 3H_2O$ has been reported.[14] The following procedure is simpler and requires much less elaborate purification steps. $RuCl_3 \cdot 3H_2O$ (200 mg, 0.76 mmol) was dissolved in ethanol (30 mL), and the solution was evaporated nearly to dryness on a steam bath. The blue residue thus produced was dissolved in ethanol (30 mL) followed by addition of HQ^1 (500 mg, 3.44 mmol) and sodium acetate (500 mg, 3.67 mmol). The whole mixture was heated to reflux for 2 h. The resulting brown solution was kept overnight in a refrigerator. The dark brown crystalline solid thus deposited was collected by filtration, washed thoroughly with hot water, and dried in vacuo over P_4O_{10}; yield 40%. Anal. Calcd for $RuC_{27}H_{18}N_3O_3$ (**3a**): C, 60.78; H, 3.38; N, 7.88. Found: C, 60.47; H, 3.41; N, 7.62.

The complex RuQ^2_3 (**3b**) was prepared (yield 50%) by an entirely analogous method using HQ^2 instead of HQ^1. Anal. Calcd for $RuC_{30}H_{24}N_3O_3$ (**3b**): C, 62.60; H, 4.17; N, 7.30. Found: C, 62.50; H, 4.18; N, 7.24.

Tris(*N*-arylsalicylaldiminato)ruthenium(III), RuL_3 (4). The following general method, which is a modification of a reported procedure, was used.[20] To a solution of *N*-arylsalicylaldimine (3.0 mmol) in ethyl benzoate (20 mL) was added tris(acetylacetonato)ruthenium(III) (0.5 mmol). The mixture was heated to 160 °C with stirring for 6 h with continuous passage of a slow stream of nitrogen through the mixture to remove volatile acetylacetone. The temperature was then lowered to 85 °C, and the solvent was removed under vacuum. The dark residue was dissolved in acetone (20 mL). This solution was filtered, and the solvent was evaporated under reduced pressure. The crude product was dissolved in a small volume of dichloromethane and was subjected to chromatography on a silica gel column (20 × 1 cm). On elution with benzene a yellow band separated out and was rejected. The next blackish green band eluted with benzene–dichloromethane (1:2) was collected and evaporated to afford a dark crystalline solid. The yield varied in the range 60–70%. Anal. Calcd for $RuC_{39}H_{30}N_3O_3$ (**4a**): C, 67.91; H, 4.35; N, 6.09. Found: C, 67.98; H, 4.30; N, 6.11. Calcd for $RuC_{42}H_{36}N_3O_3$ (**4b**): C, 68.93; H, 4.92; N, 5.74. Found: C, 68.86; H, 4.87; N, 5.66. Calcd for $RuC_{42}H_{36}N_3O_6$ (**4c**): C, 64.69; H, 4.62; N, 5.39. Found: C, 64.53; H, 4.60; N, 5.35. Calcd for $RuC_{48}H_{42}N_3O_9$ (**4d**): C, 63.64; H, 4.64; N, 4.64. Found: C, 63.59; H, 4.59; N, 4.61. Calcd for $RuC_{39}H_{27}H_3O_3Cl_3$ (**4e**): C, 59.05; H, 3.40; N, 5.30. Found: C, 59.01; H, 3.36; N, 5.28.

Doped Complexes. The doping of RuQ^1_3 in CoQ^1_3 and of RuL^1_3 in CoL^1_3 was achieved by cocrystallization of the mixtures from dichloromethane. For EPR experiments the ruthenium complex was doped to the extent of ~1%.

Tris(*N*-phenylsalicylaldiminato)ruthenium(IV) Hexafluorophosphate, $[RuL^1_3]PF_6$ (5a). **4a** (94.56 mg, 0.14 mmol) was oxidized coulometrically at 0.9 V vs SCE in acetonitrile (0.1 M NH_4PF_6). Oxidation was continued until a coulomb count equivalent to one-electron transfer accumulated. During this period the color of the solution changed from blackish green to bluish green. The solution was subjected to immediate evaporation under reduced pressure. The residue thus obtained was washed with ice-cold water and dried in vacuo over P_4O_{10}; the yield was quantitative. Anal. Calcd for $RuC_{39}H_{30}N_3O_3PF_6$ (**5a**): C, 56.11; H, 3.60; N, 5.03. Found: C, 56.21; H, 3.69; N, 5.09.

The complex $[RuL^2_3]PF_6$ (**5b**) was prepared (in quantitatie yield) similarly by using **4b** instead of **4a**. Anal. Calcd for $RuC_{42}H_{36}N_3O_3PF_6$ (**5b**): C, 57.53; H, 4.11; N, 4.79. Found: C, 57.65; H, 4.16; N, 4.85.

Dichlorobis(8-quinolinolato)osmium(IV), $OsCl_2Q^1_2$ (6a). To a suspension of $(NH_4)_2OsCl_6$ (200 mg, 0.45 mmol) in 2-methoxyethanol (50 mL) was added HQ^1 (165 mg, 1.14 mmol); the mixture was heated to reflux for 2 h, and it gradually became green. The solution was cooled and kept in the refrigerator for 2 h, affording a shining dark green crystalline precipitate, which was collected by filtration. The mass was washed thoroughly with hot water and finally with methanol. It was dried in vacuo over P_4O_{10}; yield 80%. Anal. Calcd for $OsC_{18}H_{12}N_2O_2Cl_2$ (**6a**): C, 39.35; H, 2.20; N, 5.10. Found: C, 39.42; H, 2.21; N, 5.10.

The complex $OsCl_2Q^2_2$ (**6c**; yield 85%) was prepared similarly by replacing HQ^1 by HQ^2. The bromo complexes (yield 65%) $OsBr_2Q^1_2$ (**6b**) and $OsBr_2Q^2_2$ (**6d**) were synthesized similarly from $(NH_4)_2OsBr_6$ by using HQ^1 and HQ^2, respectively. Here the reaction proceeded much faster and the reflux time was 15–30 min only. Anal. Calcd for $OsC_{20}H_{16}N_2O_2Cl_2$ (**6c**): C, 41.60; H, 2.77; N, 4.85. Found: C, 41.77; H, 2.77; N, 4.97. Calcd for $OsC_{18}H_{12}N_2O_2Br_2$ (**6b**): C, 33.87; H, 1.89; N, 4.39. Found: C, 33.96; H, 1.87; N, 4.47. Calcd for $OsC_{20}H_{16}N_2O_2Br_2$ (**6d**): C, 36.05; H, 2.42; N, 4.20. Found: C, 36.20; H, 2.50; N, 4.11.

Tetraethylammonium Dichlorobis(8-quinolinolato)osmate(III), $[Et_4N][OsCl_2Q^1_2]$ (7a). **6a** (100 mg, 0.18 mmol) was suspended in acetonitrile (50 mL) and stirred magnetically at room temperature (298 K). To this was added dropwise a methanolic solution (5 mL) of hydrazine hydrate (90 mg, 1.81 mmol). The mixture was then stirred for another 1 h. An orange-red color developed. The solution was filtered through a fine frit; to the filtrate was added $[Et_4N]Cl$ (40 mg, 0.24 mmol) was added, and the mixture was stirred magnetically for 1 h. The solution was evaporated in vacuo. The solid mass was collected and washed thoroughly with cold water. It was then dried in vacuo over P_4O_{10}; yield 90%. Anal. Calcd for $OsC_{26}H_{32}N_3O_2Cl_2$ (**7a**): C, 45.94; H, 4.74; N, 6.18. Found: C, 45.82; H, 4.71; N, 6.29.

The complexes $[Et_4N][OsBr_2Q^1_2]$ (**7b**), $[Et_4N][OsCl_2Q^2_2]$ (**7c**), and $[Et_4N][OsBr_2Q^2_2]$ (**7d**) were prepared similarly from **6b**, **6c**, and **6d**, respectively, in quantitative yield. Anal. Calcd for $OsC_{26}H_{32}N_3O_2Br_2$ (**7b**): C, 40.63; H, 4.20; N, 5.47. Found: C, 40.48; H, 4.11; N, 5.58. Calcd for $OsC_{28}H_{36}N_3O_2Cl_2$ (**7c**): C, 47.52; H, 5.13; N, 5.94. Found: C, 47.49; H, 5.18; N, 6.08. Calcd for $OsC_{28}H_{36}N_3O_2Br_2$ (**7d**): C, 42.22; H, 4.55; N, 5.27. Found: C, 42.02; H, 4.45; N, 5.39.

Tris(8-quinolinolato)osmium(III), OsQ^1_3 (8a). This compound was prepared from any one of the following species: **6a**, **6b**, **7a**, and **7b**. The details of synthesis from **6a** are described below. The other syntheses are closely similar. The yield was in the range 80–90%.

To a suspension of **6a** (100 mg, 0.182 mmol) in 2-methoxyethanol–water (40 mL, 4:1) was added HQ^1 (265 mg, 1.82 mmol), and the mixture was heated to reflux for 8 h, producing an orange-red solution, which was evaporated in vacuo. The solid mass thus obtained was washed several times with hot water to remove excess ligand. It was then dried in vacuo over P_4O_{10} and subjected to chromatography on a silica gel (60–120 mesh, BDH) column (20 × 1 cm). A small green band was first eluted with dichloromethane. Finally the slow-moving orange-red band was eluted with benzene–acetonitrile (2:1). On slow evaporation the required complex was obtained in crystalline form. Anal. Calcd for $OsC_{27}H_{18}N_3O_3$ (**8a**): C, 52.08; H, 2.91; N, 6.75. Found: C, 51.92; H, 3.01; N, 6.66.

The complex OsQ^2_3 (**8b**; yield 85%) was prepared similarly by reacting HQ^2 with any of the following chelates: **6c**, **6d**, **7c**, and **7d**. Reaction of HQ^1 with **6a** and that of HQ^2 with **6c** respectively afforded $OsQ^1_2Q^2$ (**10a**; yield 75%) and $OsQ^1Q^2_2$ (**10b**; yield 80%) by following the same procedure. Anal. Calcd for $OsC_{30}H_{24}N_3O_3$ (**8b**): C, 54.20; H, 3.64; N, 6.32. Found: C, 54.35; H, 3.71; N, 6.24. Calcd for $OsC_{28}H_{20}N_3O_3$ (**10a**): C, 52.82; H, 3.17; N, 6.60. Found: C, 52.67; H, 3.21; N, 6.52. Calcd for $OsC_{29}H_{22}N_3O_3$ (**10b**): C, 53.53; H, 3.41; N, 6.46. Found: C, 53.65; H, 3.49; N, 6.38.

Tris(8-quinolinolato)osmium(IV) Perchlorate, $[OsQ^1_3]ClO_4$ (9a). **8a** (100 mg, 0.16 mmol) was dissolved in dichloromethane–acetonitrile (20 mL, 1:1) and was stirred magnetically at room temperature (298 K). To this was added dropwise 10 mL of aqueous $Ce(SO_4)_2 \cdot 4H_2O$ (325 mg, 0.8 mmol; in 1 M H_2SO_4) solution. The orange-red solution gradually changed to green. The stirring was continued for 1 h. The solution was filtered through a fine frit. The filtrate was evaporated on a steam bath and dried. The solid mass was dissolved in acetonitrile, and to this was added a saturated aqueous solution (2 mL) of $NaClO_4$. The resulting solution was evaporated slowly in air. The crystalline precipitate was collected by filtration and washed thoroughly with ice-cold water. It was dried in vacuo over P_4O_{10} and subjected to chromatography on a silica gel (60–120 mesh, BDH) column (30 × 1 cm). A very small orange-red band was first eluted with benzene–acetonitrile (2:1). Finally the slow-moving green band was eluted with benzene–acetonitrile (3:2). On slow evaporation the crystalline compound was obtained in 90% yield. Anal. Calcd for $OsC_{27}H_{18}N_3O_7Cl$ (**9a**): C, 44.91; H, 2.51; N, 5.82. Found: C, 44.79; H, 2.45; N, 5.93.

The complex $[OsQ^2_3]ClO_4$ (**9b**; yield 85%) was prepared similarly from **8b**. Anal. Calcd for $OsC_{30}H_{24}N_3O_7Cl$ (**9b**): C, 47.15; H, 3.17; N, 5.50. Found: C, 46.97; H, 3.22; N, 5.41.

Conversions. (a) 5 → 4. **5a** (50 mg, 0.06 mmol) was reduced coulometrically at 0.4 V vs SCE in acetonitrile (0.1 M NH_4PF_6). Reduction was continued until a coulomb count equivalent to one-electron transfer accumulated. The color of the solution changed from bluish green to blackish green. The solution was evaporated on a steam bath. The mass was washed thoroughly with water and dried in vacuo over P_4O_{10}. The yield of **4a** is quantitative. The conversion **5b** → **4b** was similarly done.

(b) 7 → 6. **7a** (100 mg, 0.147 mmol) was dissolved in acetonitrile (15 mL) and stirred magnetically at room temperature (298 K). To this was added dropwise an aqueous solution of $Ce(SO_4)_2 \cdot 4H_2O$ (300 mg, 0.74 mmol; in 0.1 M H_2SO_4). The orange-red solution color gradually disappeared, and microcrystalline **6a** precipitated out. It was filtered and washed with water. The mass was extracted with dichloromethane. On slow evaporation crystalline pure **6a** was obtained; the yield was quantitative. Oxidation of **7b**, **7c**, and **7d** to **6b**, **6c**, and **6d**, respectively, was achieved similarly.

(c) 9 → 8. **9a** (100 mg, 0.138 mmol) was dissolved in acetonitrile (20 mL) and stirred magnetically at room temperature (298 K). Hydrazine hydrate (35 mg, 0.7 mmol) in acetonitrile (5 mL) was added dropwise.

The green solution changed to orange-red. The stirring was continued for 15 min. The solution was evaporated to dryness on a steam bath. The mass was washed with water and dried in vacuo over P_4O_{10}, affording **8a** in quantitative yield. Reduction of **9b** furnished **8b** similarly.

Acknowledgment. Financial support received from the Department of Science and Technology, New Delhi, India, and from the Council of Scientific and Industrial Research, New Delhi, India, is gratefully acknowledged. We are thankful to a reviewer for bringing ref 13 to our attention.

Registry No. **3a**$^+$, 111267-45-9; **3a**, 111321-91-6; **3a**$^-$, 111267-50-6; **3b**$^+$, 111267-46-0; **3b**, 111267-16-4; **3b**$^-$, 111267-51-7; **4a**$^+$, 111267-22-2; **4a**, 111267-17-5; **4a**$^-$, 111267-52-8; **4b**$^+$, 111267-24-4; **4b**, 111267-18-6; **4b**$^-$, 111267-53-9; **4c**$^+$, 111267-47-1; **4c**, 111267-19-7; **4c**$^-$, 111267-54-0; **4d**$^+$, 111267-48-2; **4d**, 111267-20-0; **4d**$^-$, 111267-55-1; **4e**$^+$, 111267-49-3; **4e**, 111267-21-1; **4e**$^-$, 111267-56-2; **5a**, 111267-23-3; **5b**, 111267-25-5; **6a**, 111267-26-6; **6a**$^{2-}$, 111267-59-5; **6b**, 111267-27-7; **6b**$^{2-}$, 111267-60-8; **6c**, 111290-88-1; **6c**$^{2-}$, 111267-61-9; **6d**, 111267-28-8; **6d**$^{2-}$, 111267-62-0; **7a**, 111267-30-2; **7b**, 111267-32-4; **7c**, 111267-34-6; **7d**, 111267-36-8; **8a**$^+$, 111267-38-0; **8a**, 111321-92-7; **8a**$^-$, 111267-63-1; **8b**$^+$, 111267-40-4; **8b**, 111267-37-9; **8b**$^-$, 111267-64-2; **9a**, 111267-39-1; **9b**, 111267-41-5; **10a**$^+$, 111267-57-3; **10a**, 111267-42-6; **10a**$^-$, 111267-65-3; **10b**$^+$, 111267-58-4; **10b**, 111267-43-7; **10b**$^-$, 111267-66-4; $Ru(acac)_3$, 14284-93-6; CoQ^1_3, 87583-61-7; CoL^1_3, 111267-44-8; $(NH_4)_2OsCl_6$, 12125-08-5; $(NH_4)_2OsBr_6$, 24598-62-7; $Ce(SO_4)_2$, 13590-82-4; N_2H_4, 302-01-2.

Contribution from the Department of Inorganic Chemistry, Indian Association for the Cultivation of Science, Calcutta 700032, India

Ionophoric Binding of Alkaline-Earth-Metal Cations (A^{2+}) by Tris(arylazo oximato)iron(II) Anions (RL^-): The Trinuclear $A(RL)_2$ Family

Samudranil Pal and Animesh Chakravorty*

Received December 30, 1986

Reaction of $NaRL\cdot H_2O$ and $A(ClO_4)_2\cdot xH_2O$ in ethanol or of HRL with ACO_3 in acetone affords $A(RL)_2$, in ≥90% yield (R = Me, Ph; A = Mg, Ca, Sr, Ba). Two complexes are formed as hydrates: $Sr(MeL)_2\cdot 4H_2O$ and $Ba(MeL)_2\cdot 5H_2O$. These furnish the anhydrous species upon heating. The $A(RL)_2$ chelates have been characterized with the help of molecular weight, IR, ^1H NMR, electrochemical, and manganese(II)-doped complex EPR data. It is concluded that in $A(RL)_2$ the A^{2+} ion is centrally held in an O_6 environment provided by the oximato oxygen atoms of the pair of facial RL^- anions (**1–3**), which act as tridentate ligands. The complexes are soluble in polar organic solvents. Quantitative ionophoric transport of 1 mol of A^{2+} from water to dichloromethane can be achieved with the help of 2 mol of PhL^-. When the aqueous phase is made acidic with 2 mol of H^+, $A(PhL)_2$ is decomposed into A^{2+} and HPhL and A^{2+} is returned to this phase. The equilibrium constants (K_{AMg}) of reactions of type $Mg(PhL)_2(o) + A^{2+}(a) \rightleftharpoons A(PhL)_2(o) + Mg^{2+}(a)$ are as follows: A = Ca, 5.10; A = Sr, 9.52; A = Ba, 24.72 (at 298 K; the abbreviations o and a signify dichloromethane and aqueous phases, respectively). This implies that the equilibrium constants K_A of reactions of type $2PhL^-(o) + A^{2+}(a) \rightleftharpoons A(PhL)_2(o)$ are in the order $K_{Ba} > K_{Sr} > K_{Ca} > K_{Mg}$. The difference ($\Delta\Delta G°_f$) of the free energies of formation of $Mg(PhL)_2$ and $A(PhL)_2$ is found to be proportional to the difference ($\Delta\Delta G°_h$) in the hydration free energies of Mg^{2+} and A^{2+} as well as to the difference ($\Delta\Delta G°_l$) of the lattice energies of crystalline MgO and AO: $\Delta\Delta G°_f/\Delta\Delta G°_h = 0.99$; $\Delta\Delta G°_f/\Delta\Delta G°_l = 0.82$.

Introduction

Ionophoric transport of alkaline-earth-metal cations (A^{2+}) from the aqueous to the organic phase is of current interest in relation to biological membrane action.[1,2] Ionophores have both polar (inside) and nonpolar (outside) regions. The polar interior binds cations, and the nonpolar exterior ensures solubility in organic phases. Oxygen donors have high affinity for A^{2+}.[3] The polar parts of most natural and synthetic A^{2+}-transporting ionophores are therefore rich in oxygen.[1,3,4] In the present work we have explored the feasibility of using the anionic complex tris(arylazo oximato)iron(II) (RL^-, **1**) for ionophoric binding of A^{2+}.

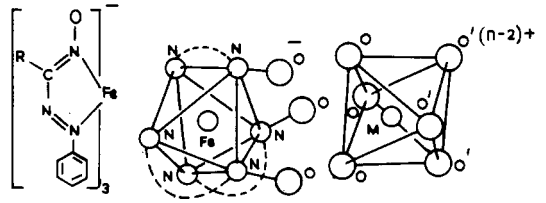

RL^-(R=Me or Ph)

1 **2** **3**

Complex **1** has the facial stereochemistry **2**.[5-7] The oximato oxygen atoms are correctly disposed to span a triangular face of another polyhedron. In other words, RL^- should be able to act as a facial O_3 ligand. Two such ligands can be aligned to define an O_6 coordination sphere as shown schematically in **3**, in which the O_3 and O'_3 faces correspond to the two ligands. This structural situation has been realized in the 3d ion (M^{n+}, n = 2, 3) complexes of type $M(RL)_2^{(n-2)+}$.[5,6]

We now report that A^{2+} can be very efficiently transported from aqueous to organic media and vice versa by utilizing the formation and decomposition of complexes of type $A(RL)_2$. A study of this phenomenon as well as the synthesis and characterization of the remarkable group of alkaline-earth-metal complexes is described.

Results and Discussion

A. Synthesis. Two methods were used for preparing $A(RL)_2$ in ≥90% yields: (i) the reaction of $NaRL\cdot H_2O$[5-7] with hydrated $A(ClO_4)_2$ in ethanol (eq 1) and (ii) reaction of HRL[7] with ACO_3

$$2NaRL + A(ClO_4)_2 \xrightarrow{EtOH} A(RL)_2 + 2NaClO_4 \quad (1)$$

$$2HRL + ACO_3 \xrightarrow{Me_2CO} A(RL)_2 + H_2O + CO_2 \quad (2)$$

suspended in boiling acetone (eq 2). The eight complexes synthesized are listed in Table I. All complexes except $Sr(MeL)_2\cdot 4H_2O$ and $Ba(MeL)_2\cdot 5H_2O$ are isolated in the anhydrous form. The two hydrated species lose water completely in a continuous thermogravimetric step over the temperature range

(1) Dietrich, B. *J. Chem. Educ.* **1985**, *62*, 954–964.
(2) Kretsinger, R. H.; Nelson, D. J. *Coord. Chem. Rev.* **1976**, *18*, 29–124. Fráusto da Silva, J. J. R.; Williams, R. J. P. *Struct. Bonding (Berlin)* **1976**, *29*, 67–121.
(3) Hubberstey, P. *Coord. Chem. Rev.* **1979**, *30*, 52–73; **1981**, *34*, 50–78; **1982**, *40*, 64–96; **1983**, *49*, 76–116; **1984**, *56*, 78–112; **1985**, *66*, 93–118; **1986**, *75*, 100–127.
(4) Katayama, Y.; Fukuda, R.; Takagi, M. *Anal. Chim. Acta* **1986**, *185*, 295–306. Cox, B. G.; Buncel, E.; Shin, H. S.; Bannard, R. A. B.; Purdon, J. G. *Can. J. Chem.* **1986**, *64*, 920–925. Sakai, Y.; Nakamura, H.; Takagi, M.; Ueno, K. *Bull. Chem. Soc. Jpn.* **1986**, *59*, 381–384.
(5) Pal, S.; Melton, T.; Mukherjee, R. N.; Chakravarty, A. R.; Tomas, M.; Falvello, L. R.; Chakravorty, A. *Inorg. Chem.* **1985**, *24*, 1250–1257.
(6) Pal, S.; Mukherjee, R. N.; Tomas, M.; Falvello, L. R.; Chakravorty, A. *Inorg. Chem.* **1986**, *25*, 200–207.
(7) Raghavendra, B. S. R.; Gupta, S.; Chakravorty, A. *Transition Met. Chem. (Weinheim, Ger.)* **1979**, *4*, 42–45.

0020-1669/87/1326-4331$01.50/0